Development 134, 901-908 (2007) doi:10.1242/dev.02783

Syne-1 and *Syne-2* play crucial roles in myonuclear anchorage and motor neuron innervation

Xiaochang Zhang[1], Rener Xu[1,*], Binggen Zhu[1], Xiujuan Yang[2], Xu Ding[1], Shumin Duan[2], Tian Xu[1,3], Yuan Zhuang[1,4] and Min Han[1,5]

Proper nuclear positioning is important to cell function in many biological processes during animal development. In certain cells, the KASH-domain-containing proteins have been shown to be associated with the nuclear envelope, and to be involved in both nuclear anchorage and migration. We investigated the mechanism and function of nuclear anchorage in skeletal muscle cells by generating mice with single and double-disruption of the KASH-domain-containing genes *Syne1* (also known as *Syne-1*) and *Syne2* (also known as *Syne-2*). We showed that the deletion of the KASH domain of Syne-1 abolished the formation of clusters of synaptic nuclei and disrupted the organization of non-synaptic nuclei in skeletal muscle. Further analysis indicated that the loss of synaptic nuclei in Syne-1 KASH-knockout mice significantly affected the innervation sites and caused longer motor nerve branches. Although disruption of neither *Syne-1* nor *Syne-2* affected viability or fertility, *Syne-1; Syne-2* double-knockout mice died of respiratory failure within 20 minutes of birth. These results suggest that the KASH-domain-containing proteins Syne-1 and Syne-2 play crucial roles in anchoring both synaptic and non-synaptic myonuclei that are important for proper motor neuron innervation and respiration.

KEY WORDS: Synaptic nuclei, Neuromuscular junction, Neonatal lethality, Nuclear envelope, KASH, SUN domain, Nesprin, ANC-1, MSP-300, Mouse

INTRODUCTION

The proper positioning of nuclei in cells is crucial for many biological processes, including fertilization, cell division, cell migration and other cell functions. Nuclear migration and anchorage have been extensively studied, and both the microtubule and the actin cytoskeleton systems have been found to play important roles in these processes (Morris, 2003; Starr and Han, 2003). In recent years, genetic analyses in several model organisms have shown that the Klarsicht/ANC-1/Syne homologue (KASH)-domain-containing proteins that are associated with the nuclear envelope play important roles in nuclear positioning during various cellular and developmental processes (Grady et al., 2005; Malone et al., 2003; Mosley-Bishop et al., 1999; Starr and Han, 2002; Starr et al., 2001; Yu et al., 2006).

The KASH domain is a conserved protein motif of approximately 60 amino acids that is located at the C-terminus of KASH-family proteins (Starr and Fischer, 2005). KASH domains have been shown to bind to nuclear envelope and are likely to be responsible for the association of the nuclear envelope with KASH proteins (Fischer et al., 2004; Grady et al., 2005; Malone et al., 2003; Starr and Han, 2002; Wilhelmsen et al., 2005; Yu et al., 2006; Zhang et al., 2001; Zhen et al., 2002). In *C. elegans*, the KASH-domain proteins UNC-83, ANC-1 and ZYG-12 have been shown to be associated with the nuclear envelope and to play roles in nuclear migration, nuclear anchorage of syncytial cells and association of centrosomes with the nuclear envelope during cell division, respectively (Hedgecock and Thomson, 1982; Horvitz and Sulston, 1980; Malone et al., 2003; Starr and Han, 2002; Starr et al., 2001). In *Drosophila*, the KASH-domain protein Klarsicht has been shown to be important for nuclear migration during eye development and for the movement of lipid droplets (Mosley-Bishop et al., 1999; Welte et al., 1998). The *Drosophila* MSP-300, a homologue of the worm ANC-1 protein in overall structure (Starr and Han, 2002; Volk, 1992; Zhang et al., 2002), was also shown to be associated with the nuclear envelope and to play a crucial role in anchoring nurse-cell nuclei during oogenesis (Yu et al., 2006).

Three KASH-domain-containing proteins have been discovered in mammals, namely Syne-1 (also known as Syne1, Myne1, Nesprin-1, Enaptin165), Syne-2 (also known as Syne2 and Nesprin-2; and as NUANCE in humans) and Nesprin-3 (Apel et al., 2000; Gough et al., 2003; Mislow et al., 2002; Padmakumar et al., 2004; Wilhelmsen et al., 2005; Zhang et al., 2001; Zhen et al., 2002). Nesprin-3 is a much smaller protein compared to the other two Syne proteins. Syne-1 and Syne-2 are orthologs of ANC-1 and MSP-300: all four proteins are very large (>6000 amino acids) and contain actin-binding domains at their N-terminus, a large middle part and a KASH domain at their C-terminus (Starr and Fischer, 2005). The KASH domains of Syne proteins have been shown to target proteins to the nuclear envelope (Apel et al., 2000; Grady et al., 2005; Zhang et al., 2001; Zhen et al., 2002). The structural similarities of Syne proteins to ANC-1 and MSP-300 suggest that they may also be involved in nuclear anchorage during important cellular and developmental processes.

Syne proteins have been implicated in playing important roles in nuclear positioning in multinucleated skeletal muscle cells. During early development of the skeletal muscle, hundreds of myoblasts fuse together to form multinucleated myotubes, and nuclei undergo migration (Englander and Rubin, 1987). Later on, each myotube matures into a large syncytial muscle fiber and nuclei are stably anchored at the periphery of each individual cell (Bruusgaard et al., 2003). Noticeably, except for a 3-8 nuclei (synaptic nuclei) cluster under the neuromuscular junction (NMJ),

[1]Institute of Developmental Biology and Molecular Medicine, School of Life Science, Fudan University, Shanghai, 200433, China. [2]Institute of Neuroscience and Key Laboratory of Neurobiology, Shanghai Institutes for Biological Sciences, Chinese Academy of Sciences, Shanghai, 200031, China. [3]Howard Hughes Medical Institute and Department of Genetics, Yale University School of Medicine, New Haven, CT 06520, USA. [4]Department of Immunology, Duke University Medical Center, Durham, NC 27706, USA. [5]Howard Hughes Medical Institute and Department of MCDB, University of Colorado, Boulder, CO 80309, USA.

*Author for correspondence (e-mail: rener_xu@fudan.edu.cn)

Accepted 14 December 2006

myonuclei distribute evenly in muscle fibers (Sanes and Lichtman, 1999). The evenly spaced localization pattern of non-synaptic nuclei is speculated to result from nuclei repelling each other to minimize the transport distance (Bruusgaard et al., 2003). However, the underlying mechanism responsible for nuclear anchorage remains unknown. In addition, synaptic nuclei have long been proposed to be transcriptionally specialized and essential in maintaining the postsynaptic components of the NMJ (Sanes and Lichtman, 2001; Schaeffer et al., 2001), but the anchoring mechanism for those nuclei has also been obscure. Both Syne-1 and Syne-2 have been found to be expressed at high levels in the skeletal muscle (Apel et al., 2000; Zhang et al., 2005; Zhang et al., 2001). More recently, a direct involvement of Syne proteins in nuclear positioning has been indicated in the study of transgenic mice expressing a dominant-negative form of Syne-1 (Grady et al., 2005). This study showed that the ectopic expression of the dominant-negative form of Syne-1 disrupted the positioning of synaptic nuclei but had no effect on the even spacing of non-synaptic nuclei. However, it remains to be determined to what degree this dominant-negative effect reflects the function of Syne proteins and which Syne protein is directly involved in myonuclear positioning during muscle development.

To thoroughly understand the cellular and physiological functions of *Syne-1* and *Syne-2*, we generated mice deficient in the KASH-domain-containing isoforms of both genes. In addition, we also generated transgenic mice that overexpress the Syne-2 KASH protein in skeletal muscle cells. We aim to understand: (1) Are KASH-domain-containing isoforms of Syne-1 and/or Syne-2 essential for the anchorage of synaptic nuclei in skeletal muscle cells? (2) Do these proteins play a role in anchoring non-synaptic nuclei? (3) Do these two homologous proteins function redundantly? and (4) What are the physiological consequences of eliminating the activities of either or both proteins?

MATERIALS AND METHODS

Generation of *Syne-1* and *Syne-2* single and double-knockout mice

The gene-targeting vectors for the *Syne-1* and *Syne-2* KASH domain were constructed from 129 genomic DNA fragments screened out of a BAC library (Invitrogen). For the *Syne-1* construct, the *Hin*dIII fragment in Fig. 1A was first cloned into pBluescript. The *Avr*II-*Hin*dIII and *Hin*dIII-*Bam*HI fragments were then cloned into pPNT at the *Not*I-*Xho*I and *Bam*HI sites, respectively. For *Syne-2*, the *Hin*dIII-*Bam*HI fragment was blunt-end ligated into the *Xho*I site of pPNT, while the *Spe*I-*Eco*RI genomic fragment was cloned into pPNT at *Xba*I-*Eco*RI. Each vector was linearized with *Not*I and electroporated into embryonic stem (ES) cells. After double selections, positive clones were screened by PCR and Southern blot, which was followed by injection to obtain chimeric mice. Chimeras and their positive progenies were backcrossed with C57/B6J mice.

Genomic DNA was extracted and genotyped using a three-primer PCR. Primers for *Syne-1* genotyping were prcmy016, prcmy017 and prcmy018 (sequence details of all primers mentioned in this paper are available upon request). Primers for *Syne-2* genotyping were prcmy019, prcmy020 and prcmy021.

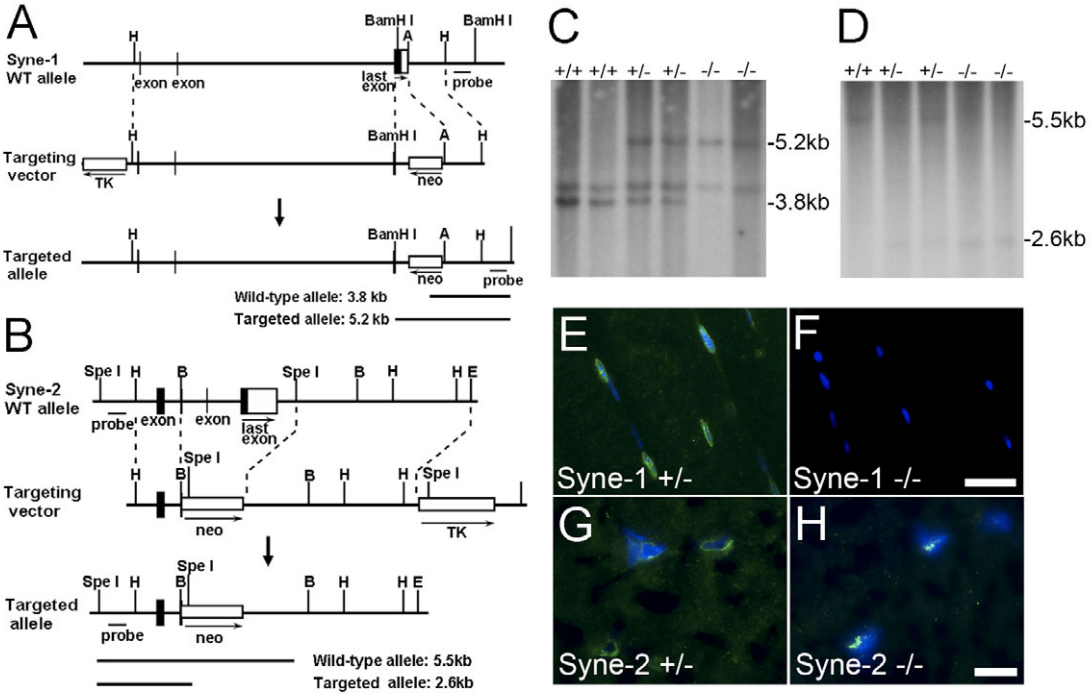

Fig. 1. The generation of Syne-1 and Syne-2 KASH-domain-deletion mice. (**A**,**B**) Schematic representation of the knockout strategies for *Syne-1* and *Syne-2*. Exons are labeled and coding regions are indicated by black boxes. In the targeting vector, the last exon of *Syne-1* (the last two exons of *Syne-2*) was replaced by a neomycin-resistance expression cassette (neo). A *HSV-TK* cassette was linked to the 5′ end (3′ end for *Syne-2*) for negative selection. Restriction enzyme sites: A, *Avr*II; B, *Bam*HI; E, *Eco*RI; H, *Hin*dIII. (**C**,**D**) Southern-blot analyses of genomic DNA from wild-type (+/+), heterozygous (+/–) and homozygous-knockout (–/–) mice. Probes used are indicated in Fig. 1A,B. (C) For *Syne-1* analysis, genomic DNA samples were digested by *Bam*HI, which yielded 3.8 kb (wild-type allele) and 5.2 kb (mutant allele) bands (notice that a 4.1 kb band caused by *Bam*HI digestion is visible in all lanes). (D) For *Syne-2*, *Spe*I-digested genomic DNA yielded 5.5 kb (wild-type allele) and 2.6 kb (mutant allele) bands. (**E-H**) Frozen sections of skeletal muscle were stained with anti-Syne-1 (green in E and F) or anti-Syne-2 (green in G and H), and DAPI (blue in all panels). Syne-1 and Syne-2 signals are visible on the nuclear envelope of samples from the control, but not the homozygous-knockout, mice. Scale bar, 25 μm in F for E,F; 10 μm in H for G,H.

Southern blot was carried out according to standard protocols (Sambrook and Russell, 2001). For *Syne-1*, genomic DNA samples were digested with *Bam*HI and hybridized with a probe obtained from the PCR amplification of C57/B6J genomic DNA with the primers XP141 and XP142. For *Syne-2*, genomic DNA samples were digested by *Spe*I and hybridized with a probe obtained from the PCR amplification of C57/B6J genomic DNA with the primers XP154 and XP155.

Generation of *Syne-2* transgenic mice

The 549 bp KASH-domain-containing fragment between *Xba*I and *Pst*I was cut from *Syne-2* cDNA (ATCC, Cat. No. 7492527) and ligated into pBluescript KS(–). A 6xMyc tag from pCS2 +MT with a 5′-end *Spe*I site was then added in frame at the N-terminus, followed by the insertion of an hGH polyA from pTWM1 to the C-terminus between the *Eco*RV and *Xho*I sites. The resulting cassette of Myc6-Syne-2 KASH-hGH polyA was then cloned into the *Spe*I and *Xho*I sites of pBMGH to position the cassette behind the MCK promoter. This vector was linearized with *Xho*I and *Sac*II before being injected into the embryos of the FVB inbred strain to obtain transgenic mice. Positive mice were identified by PCR with primers prDX032 and prDX033. Ultimately, five viable and fertile positive founders were obtained and analyzed.

Preparation of antibodies against Syne-1, Syne-2 and SUN2

DNA fragments from cDNA clones (ATCC) of *Syne-1*, *Syne-2* and *SUN2* were cloned into pET28 or pET32 after PCR amplification with the following primers: prDX059 and prDX060 for the 115 amino acid peptide at the C-terminus of Syne-1; prDX061 and prDX062 for the 66 amino acid peptide at the C-terminus of Syne-2; and prDX057 and prDX058 for the 123 amino acid peptide of SUN2. Production of recombinant proteins was induced using IPTG in *E. coli BL21* and proteins were purified using a Ni-agarose column. Polyclonal antibodies were produced by immunizing rabbits with the purified 6×His fusion proteins, and the rabbit anti-sera were affinity-purified with HiTrap NHS-activated HP columns (Amersham Bioscience).

Histological analysis

For frozen tissue sections, tissues of interest were dissected out, embedded in OCT and frozen in liquid-nitrogen-cooled isopentane. Sections (6-8 μm) were then collected.

For paraffin sections, embryos or tissues of interest were dissected out, fixed in 4% formaldehyde, dehydrated in ethanol, cleared with xylene and embedded in paraffin. Sections (5 μm) were then collected and were stained with hematoxylin and Eosin.

Immunofluorescence staining and microscopy

To analyze myonuclei of adult mice, whole-mount staining of the tibialis anterior (leg muscle) was carried out following the protocol described previously (Grady et al., 2005). The myc tag was labeled with 9E10-FITC (Sigma).

Skeletal muscle fibers of E18.5 embryos were analyzed by fixing their thoraci and then dissecting out their triangularis sterni, which were then stained with tetramethylrhodamine-conjugated α-bungarotoxin (BTX) (Molecular probes) and DAPI diluted in blocking solution (PBS containing 2% goat serum and 0.4% Triton). After thorough washing, individual fibers were teased out, mounted in mounting medium (Vectashield) and viewed under a light microscope (Misgeld et al., 2002).

To analyze branches of the phrenic nerve, diaphragms were dissected out, fixed and stained with a mixture of rabbit anti-neurofilament (Chemicon) and anti-synaptophysin (Zymed). The muscles were then washed and incubated with goat anti-rabbit IgG-FITC (Sigma), BTX and DAPI. After extensive washing, diaphragms were mounted and viewed under either a light microscope (for low magnification) or a confocal microscope for higher-resolution pictures (Leica).

Immunohistology of frozen tissue sections was carried out following standard protocols (Harlow and Lane, 1999). The following commercial antibodies were used: MuSK (Sigma), rapsyn (Sigma), synaptophysin (Zymed) and utrophin (Novocastra).

Electrophysiology

Diaphragms with intact phrenic nerves were isolated from E18.5 embryos and balanced in an oxygenated solution containing 125 mM NaCl, 2.5 mM KCl, 2 mM $CaCl_2$, 12 mM $MgCl_2$, 1.3 mM NaH_2PO_4, 25 mM $NaHCO_3$ and 10 mM glucose (pH 7.3) at room temperature. The phrenic nerve was stimulated through a suction electrode, and the diaphragm was penetrated near the main intramuscular nerve. Intracellular recordings were made with microelectrodes that measured 20-70 megaohms when filled with 3 M KCl. All data were digitized at 10 kHz and collected on magnetic disks with Axotape software (Axon Instruments).

RESULTS

Generation of *Syne-1* and *Syne-2* KASH-domain-knockout mice

To investigate the function of KASH-domain-containing Syne-1 and Syne-2 proteins in mice, we deleted each KASH domain by substituting the last exon with a neomycin-resistance cassette (Fig. 1A,B; see Materials and methods for details). After homologous recombination, each gene was predicted to have a premature translation-termination codon and form a truncated protein. Gene targeting was carried out in 129 ES cells and the chimeras were crossed with C57/B6J mice. Homologous recombination in mice was confirmed by PCR and Southern blot (Fig. 1C,D and data not shown), and the homozygous-knockout mice of either *Syne-1* or *Syne-2* were viable and fertile.

To further confirm that the KASH domains were eliminated in these mutants, we first carried out reverse transcriptase (RT)-PCR with total mRNA from both heart and skeletal muscle, and found that the coding sequence for each KASH domain could not be amplified, whereas a middle segment of each gene was transcribed (data not shown). Secondly, we used immunofluorescence staining to examine nuclear envelope-localized Syne proteins with antibodies against the C-terminal part of each protein (see Materials and methods). Both Syne-1 and Syne-2 were found to localize to the

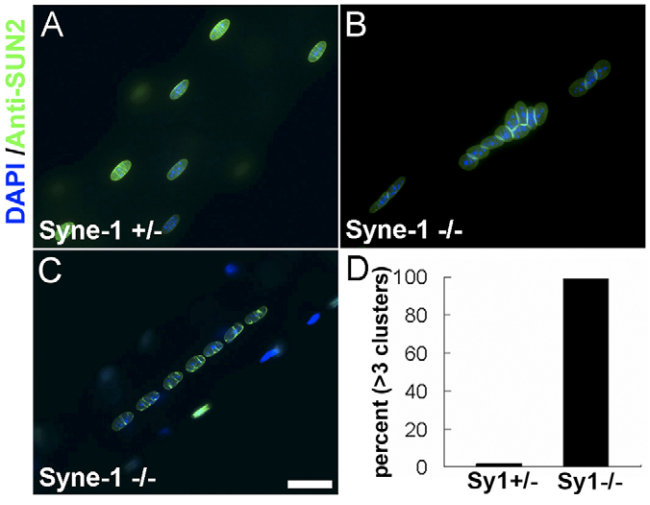

Fig. 2. Non-synaptic nuclei are disorganized in *Syne-1*$^{-/-}$ mice. (**A-C**) A single muscle fiber was teased from the tibialis anterior and simultaneously stained with DAPI (blue) and anti-SUN2 (green). Myonuclei were found to be distributed evenly in *Syne-1*$^{+/-}$ (A), but formed clusters (B) and arrays (C) in *Syne-1*$^{-/-}$ mice. (**D**) Statistical data shows that more than 99% of fibers in *Syne-1*$^{-/-}$ mice formed three or more nuclear clusters outside NMJs (n>110 for each group). Scale bar: 25 μm.

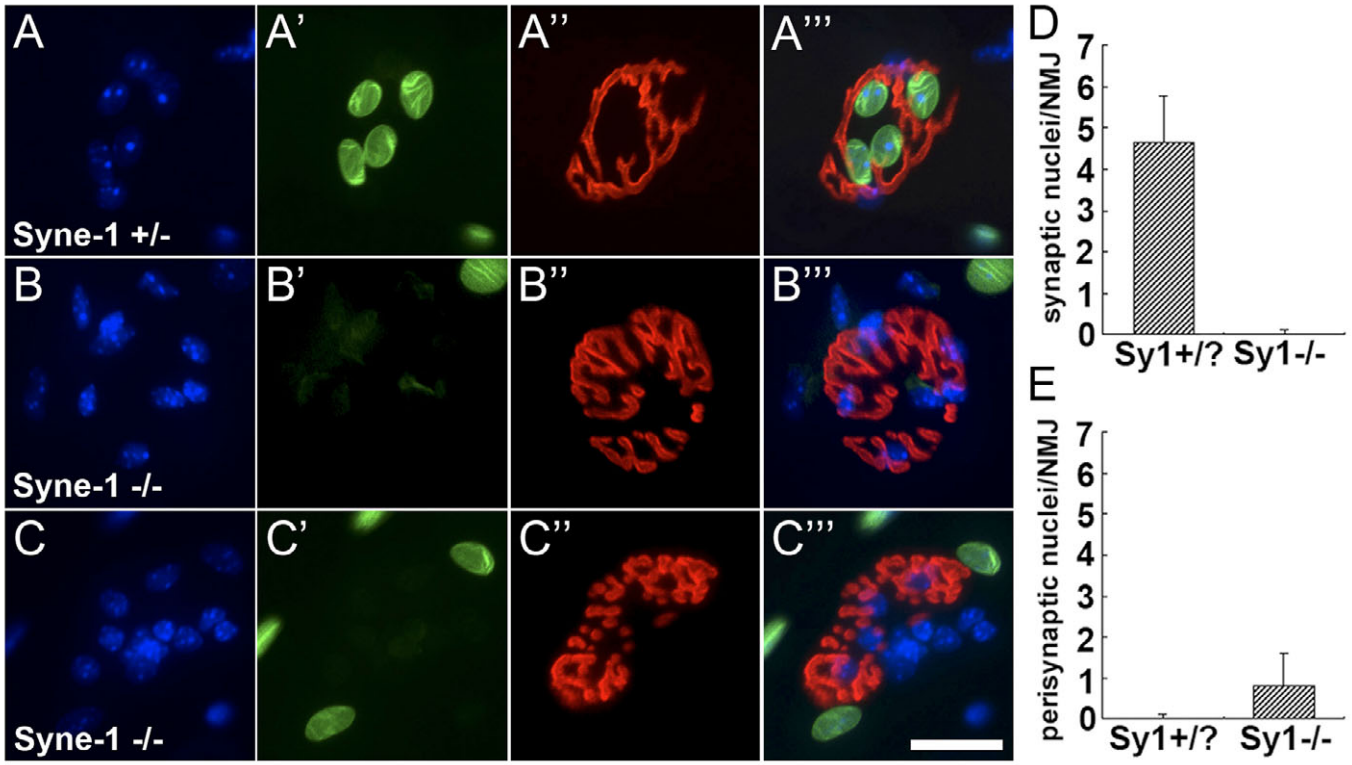

Fig. 3. **Anchorage of synaptic nuclei is abolished in *Syne-1*$^{-/-}$ mice.** (**A-A‴**) Representative *Syne-1*$^{+/-}$ muscle fiber with four nuclei (synaptic nuclei) clustered under the NMJ. (**B-C‴**) No nuclei were observed under the NMJ of *Syne-1*$^{-/-}$ mice. (**D**,**E**) Statistical analyses of synaptic nuclei based on anti-SUN2 signals. Synaptic nuclei disappeared in *Syne-1*$^{-/-}$ mice (4.7 in *Syne-1*$^{+/+}$ and *Syne-1*$^{+/-}$ vs 0.0 in *Syne-1*$^{-/-}$, n=140 for *Syne-1*$^{+/?}$ and 210 for *Syne-1*$^{-/-}$, P<0.0001); the number of perisynaptic nuclei was slightly increased in *Syne-1*$^{-/-}$ mice (0.0 in control vs 0.8 in KO, P<0.0001). Blue, DAPI; Green, anti-SUN2-labeled myonuclei; Red, BTX. Scale bar: 25 μm.

nuclear envelope in heterozygous skeletal muscle but not in homozygous-mutant mice (Fig. 1E-H). We concluded that we had established Syne-1 and Syne-2 KASH-domain-knockout mice, referred to as *Syne-1*$^{-/-}$ and *Syne-2*$^{-/-}$ mice, respectively.

Non-synaptic nuclei are disorganized in *Syne-1*$^{-/-}$ mice

Previous work using transgenic mice overexpressing the KASH domain of Syne-1 did not detect obvious defects in non-synaptic-nuclei organization in syncytial skeletal muscle cells (Grady et al., 2005), but the dominant-negative effect of the transgene was not sufficient to eliminate the endogenous Syne-1 protein from the nuclear envelope. We thus analyzed nuclei positioning in syncytial skeletal muscle cells in *Syne-1*$^{-/-}$ mice. In order to exclude the interference of nuclei from connective tissues and Schwann cells outside muscle cells when DAPI staining was used, we employed an anti-SUN2 antibody as an additional marker to label myonuclei, as the antibody specifically recognizes the nuclear envelope of skeletal muscle cells (Fig. 2A-C, and see text below; unpublished data from X.D.).

In wild-type mice, non-synaptic nuclei distribute uniformly along the whole muscle fiber (Fig. 2A). By marked contrast, nuclei clustered together abnormally in *Syne-1*$^{-/-}$ mice (a nuclear cluster was defined as three or more nuclei grouped together, with the distance between adjacent nuclei less than their diameter) (Fig. 2B,C). Statistical data showed that over 99% of *Syne-1*$^{-/-}$ muscle fibers contained more than three nuclear clusters (Fig. 2D). These results indicate that myonuclei lacking anchorage float freely in *Syne-1*$^{-/-}$ mice, and that Syne-1 is essential to properly anchor non-synaptic nuclei and to create the space between them.

Anchorage of synapse-associated nuclei is abolished in *Syne-1*$^{-/-}$ mice

Syne-1 has been shown to be concentrated at synaptic nuclei (Apel et al., 2000). In previous analysis using transgenic mice expressing the C-terminus of Syne-1, the number of synaptic nuclei was drastically reduced while the number of nuclei peripheral to synapse was almost equally increased so that the total number of nuclei associated with a synapse was essentially unchanged (Grady et al., 2005). Given the caveats of the dominant-negative effect of this transgene, as mentioned earlier, it is essential to examine *Syne-1*$^{-/-}$ mice to understand the role of *Syne-1* in synaptic-nuclei positioning.

We stained muscle fibers with BTX (marking the AChRs) and labeled myonuclei simultaneously with DAPI and anti-SUN2. In this study, we followed the methods of Grady et al. (Grady et al., 2005) to define a nucleus to be synaptic or perisynaptic: a nucleus was defined as synaptic when at least 25% of the DAPI and SUN2 signal overlapped with the BTX-positive site, and a perisynaptic nucleus was counted if the DAPI and SUN2 signal did not overlap with the BTX-positive site but was less than half its diameter from the edge of a site. Statistical data based on DAPI staining demonstrated that the number of synaptic nuclei was significantly reduced (data not

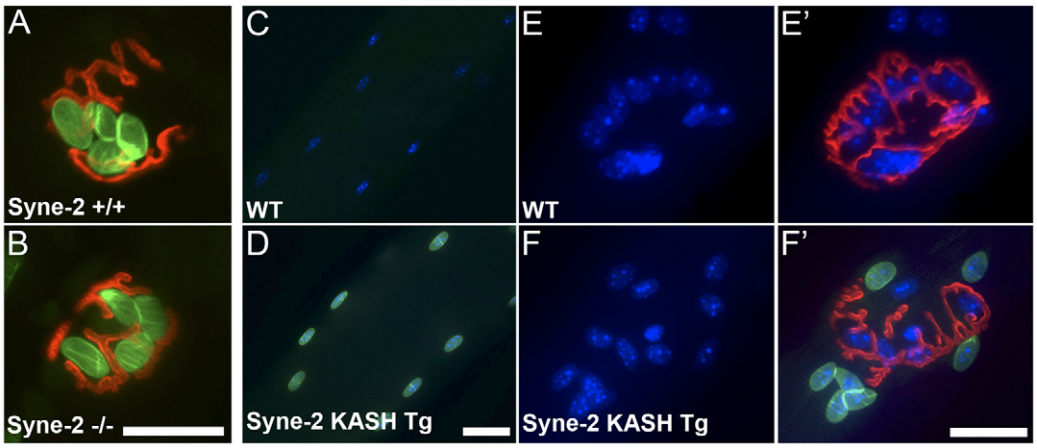

Fig. 4. Myonuclei positioning is not affected in *Syne-2*$^{-/-}$ mice, but an MCK-driven Syne-2 KASH transgenic protein displays a dominant-negative effect. (**A**,**B**) Anchorage of synaptic nuclei in *Syne-2*$^{-/-}$ mice (B) was similar to wild-type mice (A). Green, anti-SUN2 labeled myonuclei; red, BTX. (**C**,**D**) An MCK-promoter-driven C-terminal fragment of Syne-2 containing the KASH domain was localized to the nuclear envelope in skeletal muscle cells (D). Blue, DAPI; green, anti-myc. (**E-F′**) Overexpressed Syne-2 KASH fragment expelled synaptic nuclei from under the NMJ to the peripheral region (F,F′), compared with wild-type (E,E′). Noticeably, myonuclei expressing the transgene (green) rarely stayed under synapses (F′). Scale bars: 25 μm in B for A,B; 25 μm in C for C,D; 25 μm in F for E-F′.

shown). However, considering the potential noise of non-muscle cell nuclei stained by DAPI, we further analyzed nuclear positioning based on SUN2 signals.

In wild-type and *Syne-1*$^{+/-}$ mice, there were, on average, approximately 4-5 nuclei clustered under each NMJ (n=140) (Fig. 3A‴). By contrast, no nuclei were seen under the NMJ in *Syne-1*$^{-/-}$ mice (n=210, P<0.0001; Fig. 3B‴,C‴,D). This defect is significantly more severe than the previous observation using *MCK-Syne-1 KASH* transgenic mice, where 1.5 nuclei on average were still observed under the NMJ (Grady et al., 2005). Surprisingly, there was an average of only 0.8 perisynaptic nuclei in *Syne-1*$^{-/-}$ mice, compared with zero in their littermate controls (P<0.0001; Fig. 3). In *MCK-Syne-1 KASH* transgenic mice, this average was greater than 2.5 nuclei (Grady et al., 2005). Therefore, the total number of synapse-associated nuclei (synaptic nuclei plus perisynaptic nuclei) was dramatically reduced in *Syne-1*$^{-/-}$ mice [0.8 in *Syne-1*$^{-/-}$ vs 4.7 in wild type (P<0.0001), compared with 5.0 in *Syne-1 KASH* transgenic mice]. Furthermore, the anchorage defects of myonuclei in *Syne-1*$^{-/-}$ mice were repeatedly observed in different pieces of skeletal muscle, including in the diaphragm, tibialis anterior and triangularis sterni. These observations indicate that *Syne-1* plays a crucial role in the positioning of synaptic nuclei in skeletal muscle.

Myonuclear positioning in *Syne-2*$^{-/-}$ mice is normal, but an MCK-driven Syne-2 KASH transgenic protein displays a dominant-negative effect

Syne-2 has a similar protein structure to Syne-1 and, like Syne-1, is also expressed in skeletal muscle (Apel et al., 2000; Starr and Han, 2002; Zhang et al., 2001; Zhen et al., 2002). Using the same methods described above, we found that both synaptic nuclei and non-synaptic nuclei were properly positioned in *Syne-2*$^{-/-}$ mice (Fig. 4B and data not shown). Thus, Syne-2 alone is not essential for the myonuclear positioning process.

To examine a potential overlapping function of Syne-2 with that of Syne-1 in the anchoring of myonuclei, we generated transgenic mice carrying the KASH fragment of Syne-2 driven by the MCK promoter (Jaynes et al., 1988). In all five lines that we obtained, the transgenic protein was localized to the nuclear envelope in skeletal muscle, whereas endogenous Syne-1 at the nuclear envelope was significantly decreased in two lines where the transgene was highly expressed (Fig. 4D and data not shown). Additionally, in those two lines, nuclei carrying transgenic Syne-2 rarely stayed under the NMJ, and synaptic nuclei were expelled from under the NMJ to the peripheral region (Fig. 4F′). Thus, the Syne-2 fragment that contained the KASH domain displayed a similar dominant-negative effect to that of Syne-1 (Grady et al., 2005). Those results indicate that Syne-1 and Syne-2 might share the same docking sites on the nuclear envelope and that Syne-2 could play a regulatory role in the anchoring of myonuclei.

Syne-1 and Syne-2 KASH-domain double-knockout mice fail to breathe and die shortly after birth

The conserved protein structure between Syne-1 and Syne 2, their overlapping expression patterns and the above results in Syne-2 transgenic mice suggest that *Syne-1* and *Syne-2* may have redundant functions. Thus, we examined the consequences of deleting both KASH domains. *Syne-1*- and *Syne-2*-homozygous mutants were crossed to generate double-heterozygous mice, which were then crossed to produce *Syne-1*$^{+/-}$*; Syne-2*$^{-/-}$ and *Syne-1*$^{-/-}$*; Syne-2*$^{+/-}$ mice. The Syne double-heterozygous, *Syne-1*$^{+/-}$*; Syne-2*$^{-/-}$ and *Syne-1*$^{-/-}$*; Syne-2*$^{+/-}$ mice were viable and fertile. *Syne-1*$^{+/-}$*; Syne-2*$^{-/-}$ and *Syne-1*$^{-/-}$*; Syne-2*$^{+/-}$ mice were then inter-crossed to obtain *Syne-1*$^{-/-}$ *and Syne-2*$^{-/-}$ double-homozygous-knockout (referred to hereafter as *Syne* DKO) mice. Although *Syne-1*$^{+/-}$*; Syne-2*$^{+/-}$, *Syne-1*$^{-/-}$*; Syne-2*$^{+/-}$ and *Syne-1*$^{+/-}$*; Syne-2*$^{-/-}$ mice were born at percentages consistent with the expected Mendelian ratio, we could not obtain viable *Syne* DKO mice when genotyping at or after postnatal day 7.

Careful analysis indicated that *Syne* DKO mice were born alive but died within 20 minutes and were soon cannibalized by the mothers. While these double-homozygous pups had a similar body weight and anatomy to their littermates, they were cyanotic at birth and unable to breathe even though they were able to open the mouth (Fig. 5B and data not shown). Their hearts beat for a few minutes

prior to death. In addition, the *Syne* DKO babies could move their legs in response to a painful stimulus, but failed to move their ribcages. Postmortem histological analysis of the lungs demonstrated that the alveoli air sacs of these mice were not expanded (Fig. 5F), although their skeletal muscle displayed grossly normal architecture (Fig. 5C,D).

The robust lethal phenotype of *Syne* DKO mice indicates that a minimum of one copy of either *Syne-1* or *Syne-2* is required to perform an essential function immediately after birth. Considering the potential role of *Syne-2* in the positioning of myonuclei, we examined the anchorage of synaptic nuclei in *Syne* DKO mice and their littermates at E18.5 (Fig. 6). Although *Syne-1*$^{+/-}$*; Syne-2*$^{-/-}$ and *Syne-1*$^{+/-}$*; Syne-2*$^{+/-}$ mice had similar numbers of synaptic nuclei (nearly one nuclei per NMJ for both strains), the nuclei associated with every synapse were essentially eliminated in *Syne-1*$^{-/-}$*; Syne-2*$^{+/-}$ mice (average of 0.0 per NMJ, n=85). However, the synaptic-nuclei number of *Syne* DKO mice was similar to that of *Syne-1*$^{-/-}$*; Syne-2*$^{+/-}$ mice (0.0 vs 0.0, n=165 for *Syne* DKO and n=85 for *Syne-1*$^{-/-}$*; Syne-2*$^{+/-}$ mice, P>0.1 by Student's t-test). Therefore, the synaptic-nuclear-anchorage defect alone is not sufficient to account for the lethality.

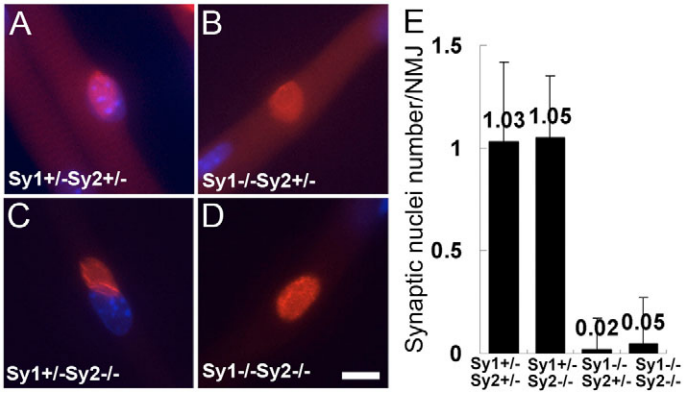

Fig. 6. Nuclear-anchorage defects in muscle of *Syne* DKO mice. (**A-D**) Representative NMJs from E18.5 triangularis sterni of the four different *Syne*-knockout genotypes. Sy1 and Sy2 represent *Syne-1* and *Syne-2*, respectively. Blue, DAPI; red, BTX. Notice that one synaptic nucleus (blue) stayed under the NMJ (red) in A and C, but not in B or D. (**E**) Statistical data showed that the *Syne-1*$^{-/-}$*; Syne-2*$^{+/-}$ and *Syne* DKO embryos displayed a significant loss of synaptic nuclei compared with embryos of the other two genotypes. Scale bar: 10 μm.

Phrenic nerves display longer branches in *Syne-1*$^{-/-}$ and *Syne* DKO mutants

The neonatal-lethality or lack-of-breathing phenotype of DKO mice may be due to the malfunction of motor neurons, possibly resulting from the loss of synaptic nuclei in skeletal muscle cells. We therefore examined whether a loss of synaptic myonuclei affected the nerve-branching process in the diaphragm, which is controlled by phrenic nerves and plays an essential role in breathing. At E18.5, branches of phrenic nerves in *Syne-1*$^{+/-}$*; Syne-2*$^{-/-}$ mice were similar to that of *Syne-1*$^{+/-}$*; Syne-2*$^{+/-}$ mice, but both *Syne-1*$^{-/-}$*; Syne-2*$^{+/-}$ and *Syne* DKO mice exhibited significantly longer branches than the double-heterozygous control (Fig. 7A-D, n>10 for each group). On the other hand, the AChR bands co-localized with synapses of phrenic nerves in all four genotypes (Fig. 7A′-D′). Therefore, *Syne* DKO mice and *Syne-1*$^{-/-}$*; Syne-2*$^{+/-}$ mice displayed significantly broader endplate bands than their littermates.

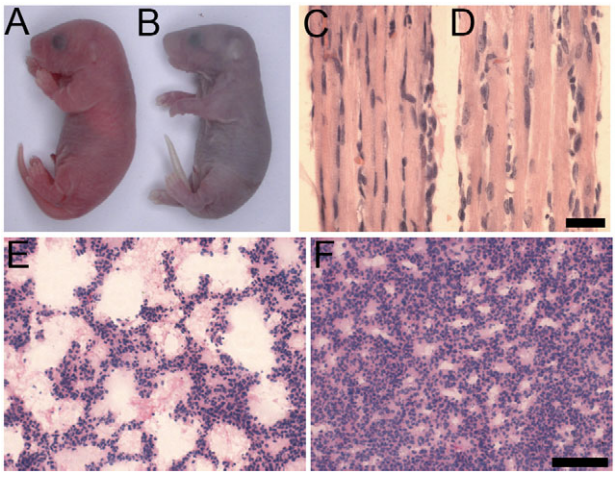

Fig. 5. *Syne-1* and *Syne-2* double-knockout mice die soon after birth. (**A**,**B**) Newborn *Syne* DKO mice (B) appeared cyanotic at birth compared to their double-heterozygous littermates (A). (**C**,**D**) Longitudinal sections of E18.5 diaphragms. *Syne* DKO embryo displayed grossly normal muscle anatomy (D) compared to *Syne-1*$^{+/-}$*; Syne-2*$^{+/-}$ (C). (**E**,**F**) Postmortem histological analysis of the lung showed that the alveoli air sacs of DKO mice were not expanded (F), indicating the failure of breathing. A *Syne-1*$^{+/-}$*; Syne-2*$^{+/-}$ littermate was used as the control (E). Scale bars: 25 μm in D for C,D; 100 μm in F for E,F.

DISCUSSION

Syne-1, Syne-2, SUN proteins and nuclear positioning in skeletal muscle

A previous study showed that overexpressing the Syne-1 C-terminus, which includes the KASH domain, in mouse skeletal muscle blocked the localization of the majority of endogenous Syne-1 to the nuclear envelope and expelled synaptic nuclei from under the NMJ to the peripheral region (Grady et al., 2005). However, no severe physiological defects were observed to accompany the cellular disorder, and the anchorage of non-synaptic nuclei appeared normal in these transgenic animals. Because the dominant-negative effect of the transgene reduced but did not eliminate Syne-1 proteins from the nuclear envelope, it was thus not clear to what extent the Syne-1 protein is required for nuclear anchorage in muscle cells. Additionally, because both Syne-1 and Syne-2 are expressed in skeletal muscle cells and both could interact with the same SUN proteins to mediate localization to the nuclear envelope, it is not clear whether the dominant-negative effect of overexpressing the KASH domain of Syne-1 is specific to the *Syne-1* gene. Our result that the expression of the KASH fragment of Syne-2 displayed a similar dominant-negative effect to that of Syne-1 (Fig. 4) further raised this concern and indicates the importance of carrying out analysis using loss-of-function alleles.

Syne-1$^{-/-}$ mice displayed an almost complete loss of synaptic nuclei, which was far more severe than that described in the previous transgenic study (Grady et al., 2005). The difference may be caused by the low level of nuclear envelope-associated endogenous Syne-1 in the transgenic mice, which was sufficient to trap the migrating myonuclei at the postsynaptic region, but was not sufficient to stably anchor them when the muscle underwent violent contractions. In *Syne-1*$^{-/-}$ mice, both the trapping and the anchorage processes were disrupted.

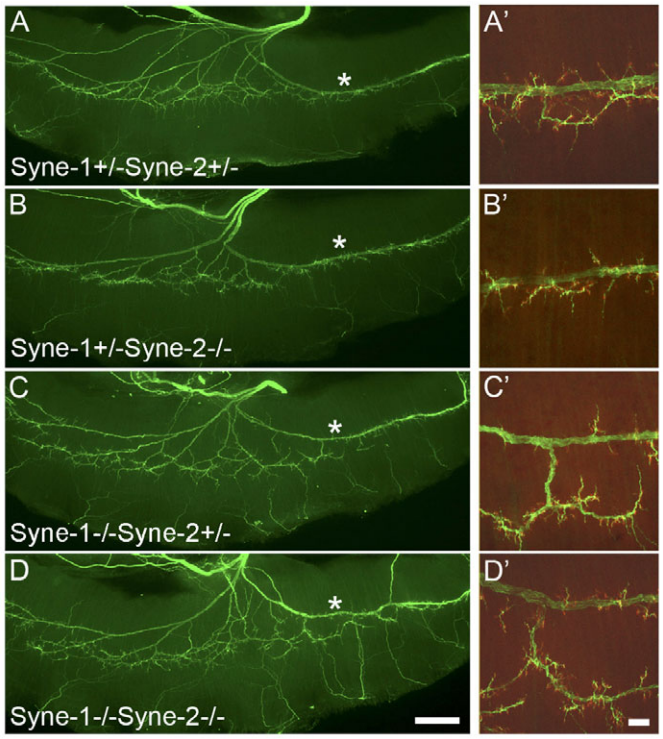

Fig. 7. Phrenic nerves display longer branches in *Syne-1*$^{-/-}$ and *Syne* DKO mutants. (**A-D**) Whole-mount diaphragms of E18.5 embryos were stained with anti-neurofilament and anti-synaptophysin (green). The right hemi-diaphragm of each genotype is shown. Longer branches are obvious in *Syne-1*$^{-/-}$*; Syne-2*$^{+/-}$ and *Syne-1*$^{-/-}$*; Syne-2*$^{-/-}$ samples. (**A'-D'**) Enlarged views of asterisk-indicated regions in A-D, showing the elongated phrenic nerve branches (green) and the broader endplate bands (red) in *Syne-1*$^{-/-}$*; Syne-2*$^{+/-}$ and *Syne-1*$^{-/-}$*; Syne-2*$^{-/-}$ diaphragms (C',D'). Scale bars: 500 μm in D for A-D; 50 μm in D' for A'-D'.

Strikingly, we found that *Syne-1* is crucial for the positioning of not only synaptic nuclei, but also of non-synaptic nuclei. In addition, approximately 2% of the muscle cells of *Syne-1*$^{-/-}$ mice exhibited centralized nuclei, compared with less than 0.5% in the control group (see Fig. S1 in the supplementary material). The severely disrupted organization of non-synaptic nuclei could impair normal nuclear-cytoplasm transportation, as well as other interactions, in the large syncytial muscle cells. This could then cause the weakening of the normal functions of skeletal muscle. This important phenotype was not observed in the previous transgenic mice expressing the KASH fragment of Syne-1 (Grady et al., 2005), again indicating that there was still a considerable level of Syne-1 on the nuclear envelope that was sufficient to anchor the myonuclei in the transgenic mice.

The dominant-negative effect caused by the Syne-2 KASH transgene (Fig. 4) and the expression of Syne-2 in muscle cells supports the hypothesis that Syne-2 could have overlapping functions with Syne-1 and that both proteins are likely to interact with a common factor for their nuclear envelope localization (see below). However, the differences between the phenotypes of the two single-knockout mice indicate that *Syne-1* plays a much more prominent role in myonuclei anchorage than does *Syne-2*.

C. elegans SUN-domain-containing proteins (e.g. UNC-84, SUN-1) have been shown to play important roles in nuclear positioning by recruiting KASH-domain proteins to the nuclear envelope (Malone et al., 2003; Starr et al., 2001). In tissue-culture cells, Syne-1 and Syne-2 have also been shown to localize to the nuclear envelope in a SUN-domain-protein-dependent manner (Crisp et al., 2006; Padmakumar et al., 2005) (X.D. and X.Z., unpublished data). Thus, mouse SUN1 and SUN2 are likely to be the partners of Syne proteins and probably play roles in myonuclear anchorage.

Synaptic nuclei and NMJ development

Synaptic nuclei have long been proposed to be transcriptionally specialized to maintain the postsynaptic components (see Introduction), but the importance of those nuclei has never been studied in mutant mice that lacked them. *Syne-1*$^{-/-}$ and *Syne* DKO mice provide an effective model system to study this issue. Surprisingly, neither presynaptic (synaptophysin) nor postsynaptic (AChR, rapsyn, MuSK and utrophin) components were found to be obviously depleted from the NMJs of *Syne* DKO mutants (see Fig. S2 in the supplementary material). In addition, the termini of phrenic nerves, which were labeled with a mixture of anti-synaptophysin and anti-neurofilament, co-localized well with AChR patches in E18.5 *Syne* DKO embryos (data not shown). These results suggest that the Agrin-MuSK-Rapsn pathway, which is crucial for the development of the NMJ (DeChiara et al., 1996; Gautam et al., 1995), is not obviously affected in *Syne-1*$^{-/-}$ or *Syne* DKO mice.

However, given that NMJ-specific genes were not completely depleted, the loss of synaptic nuclei might reduce the expression level of those genes and weaken the normal functions of the NMJ. Consistent with this notion, we observed that the phenic nerves displayed longer branches in both *Syne-1*$^{-/-}$ and *Syne* DKO mice. Therefore, synaptic nuclei may play important roles in selecting or maintaining the innervation sites by strengthening the communication between nerve and muscle at the newly formed muscle-nerve contacts.

The cause of neonatal lethality of *Syne* DKO mice

Because we failed to identify major differences in the muscle morphology, NMJ structure and motor-nerve branching between the *Syne-1*$^{-/-}$*; Syne-2*$^{+/-}$ and the *Syne* DKO embryos, we carried out an electrophysiological experiment and examined the endplate potential (EPP) to find out whether the neuromuscular transmission was blocked in *Syne* DKO mutants. However, the paired-pulse ratio and the decay of the evoked EPP in E18.5 *Syne* DKO diaphragms showed no significant difference from that of the *Syne-1*$^{-/-}$*; Syne-2*$^{+/-}$ embryos (see Fig. S3 in the supplementary material). This result suggests that the NMJ in *Syne* DKO mutants may remain functional in transmitting synaptic potentials from a motor neuron terminal to its corresponding muscle cell. The neonatal *Syne* DKO mutants may die of downstream defects inside the skeletal muscle cells, such as the intracellular-Ca^{2+} mobilization and the excitation-contraction coupling of the muscle.

Thus, the cause of the respiration failure and lethality associated with *Syne* DKO mice remains obscure. Although the observed neonatal lethality may be due to an unknown cellular function associated with the two Syne proteins, such as defects during the development of the central nervous system, it is still conceivable that the additive effects that knocking out both genes has on disrupting nuclear anchorage is the fundamental cause of the fatality.

We thank Xiaohui Wu, Yanling Yang and Yanfeng Tan for help in making chimeras and transgenic mice; Wanhua Shen and Xiumei Wu for help in setting up the electrophysiological experiment and for analyzing data; Muyun Chen for help in generating antibodies; Beibei Ying, Xiaohui Wu, Kejing Deng, Lin Sun and Wufan Tao for help in multiple aspects of this work; R. Mark Grady, Joshua R. Sanes, Zhengge Luo and Lin Mei for antibodies and helpful suggestions; Yuliang Shi, Xiongli Yang, Hai Huang, Jian Liu, Yin Shen, Lihao

Ge, Guoyuan Liu, Min Wan, Mingyao Ying and members of IDM for technical help and valuable discussions; and Diana Ronai and Aileen Sewell for comments on the manuscript. This work was supported by grants from the National Natural Science Foundation of China, Shanghai Municipal Government (Division of Science and Technology) and Morgan-Tan Center of Life Science (Fudan).

Supplementary material

Supplementary material for this article is available at http://dev.biologists.org/cgi/content/full/134/5/901/DC1

References

Apel, E. D., Lewis, R. M., Grady, R. M. and Sanes, J. R. (2000). Syne-1, a dystrophin- and Klarsicht-related protein associated with synaptic nuclei at the neuromuscular junction. *J. Biol. Chem.* **275**, 31986-31995.

Bruusgaard, J. C., Liestol, K., Ekmark, M., Kollstad, K. and Gundersen, K. (2003). Number and spatial distribution of nuclei in the muscle fibres of normal mice studied in vivo. *J. Physiol.* **551**, 467-478.

Crisp, M., Liu, Q., Roux, K., Rattner, J. B., Shanahan, C., Burke, B., Stahl, P. D. and Hodzic, D. (2006). Coupling of the nucleus and cytoplasm: role of the LINC complex. *J. Cell Biol.* **172**, 41-53.

DeChiara, T. M., Bowen, D. C., Valenzuela, D. M., Simmons, M. V., Poueymirou, W. T., Thomas, S., Kinetz, E., Compton, D. L., Rojas, E., Park, J. S. et al. (1996). The receptor tyrosine kinase MuSK is required for neuromuscular junction formation in vivo. *Cell* **85**, 501-512.

Englander, L. L. and Rubin, L. L. (1987). Acetylcholine receptor clustering and nuclear movement in muscle fibers in culture. *J. Cell Biol.* **104**, 87-95.

Fischer, J. A., Acosta, S., Kenny, A., Cater, C., Robinson, C. and Hook, J. (2004). Drosophila klarsicht has distinct subcellular localization domains for nuclear envelope and microtubule localization in the eye. *Genetics* **168**, 1385-1393.

Gautam, M., Noakes, P. G., Mudd, J., Nichol, M., Chu, G. C., Sanes, J. R. and Merlie, J. P. (1995). Failure of postsynaptic specialization to develop at neuromuscular junctions of rapsyn-deficient mice. *Nature* **377**, 232-236.

Gough, L. L., Fan, J., Chu, S., Winnick, S. and Beck, K. A. (2003). Golgi localization of Syne-1. *Mol. Biol. Cell* **14**, 2410-2424.

Grady, R. M., Starr, D. A., Ackerman, G. L., Sanes, J. R. and Han, M. (2005). Syne proteins anchor muscle nuclei at the neuromuscular junction. *Proc. Natl. Acad. Sci. USA* **102**, 4359-4364.

Harlow, E. and Lane, D. (1999). *Using Antibodies: A Lab Manual*. Cold Spring Harbor: Cold Spring Harbor Laboratory Press.

Hedgecock, E. M. and Thomson, J. N. (1982). A gene required for nuclear and mitochondrial attachment in the nematode Caenorhabditis elegans. *Cell* **30**, 321-330.

Horvitz, H. R. and Sulston, J. E. (1980). Isolation and genetic characterization of cell-lineage mutants of the nematode Caenorhabditis elegans. *Genetics* **96**, 435-454.

Jaynes, J. B., Johnson, J. E., Buskin, J. N., Gartside, C. L. and Hauschka, S. D. (1988). The muscle creatine kinase gene is regulated by multiple upstream elements, including a muscle-specific enhancer. *Mol. Cell. Biol.* **8**, 62-70.

Malone, C. J., Misner, L., Le Bot, N., Tsai, M. C., Campbell, J. M., Ahringer, J. and White, J. G. (2003). The C. elegans hook protein, ZYG-12, mediates the essential attachment between the centrosome and nucleus. *Cell* **115**, 825-836.

Misgeld, T., Burgess, R. W., Lewis, R. M., Cunningham, J. M., Lichtman, J. W. and Sanes, J. R. (2002). Roles of neurotransmitter in synapse formation: development of neuromuscular junctions lacking choline acetyltransferase. *Neuron* **36**, 635-648.

Mislow, J. M., Kim, M. S., Davis, D. B. and McNally, E. M. (2002). Myne-1, a spectrin repeat transmembrane protein of the myocyte inner nuclear membrane, interacts with lamin A/C. *J. Cell Sci.* **115**, 61-70.

Morris, N. R. (2003). Nuclear positioning: the means is at the ends. *Curr. Opin. Cell Biol.* **15**, 54-59.

Mosley-Bishop, K. L., Li, Q., Patterson, L. and Fischer, J. A. (1999). Molecular analysis of the klarsicht gene and its role in nuclear migration within differentiating cells of the Drosophila eye. *Curr. Biol.* **9**, 1211-1220.

Padmakumar, V. C., Abraham, S., Braune, S., Noegel, A. A., Tunggal, B., Karakesisoglou, I. and Korenbaum, E. (2004). Enaptin, a giant actin-binding protein, is an element of the nuclear membrane and the actin cytoskeleton. *Exp. Cell Res.* **295**, 330-339.

Padmakumar, V. C., Libotte, T., Lu, W., Zaim, H., Abraham, S., Noegel, A. A., Gotzmann, J., Foisner, R. and Karakesisoglou, I. (2005). The inner nuclear membrane protein Sun1 mediates the anchorage of Nesprin-2 to the nuclear envelope. *J. Cell Sci.* **118**, 3419-3430.

Sambrook, J. and Russell, D. (2001). *Molecular Cloning: A Laboratory Manual* (3rd edn). Cold Spring Harbor: Cold Spring Harbor Laboratory Press.

Sanes, J. R. and Lichtman, J. W. (1999). Development of the vertebrate neuromuscular junction. *Annu. Rev. Neurosci.* **22**, 389-442.

Sanes, J. R. and Lichtman, J. W. (2001). Induction, assembly, maturation and maintenance of a postsynaptic apparatus. *Nat. Rev. Neurosci.* **2**, 791-805.

Schaeffer, L., de Kerchove d'Exaerde, A. and Changeux, J. P. (2001). Targeting transcription to the neuromuscular synapse. *Neuron* **31**, 15-22.

Starr, D. A. and Han, M. (2002). Role of ANC-1 in tethering nuclei to the actin cytoskeleton. *Science* **298**, 406-409.

Starr, D. A. and Han, M. (2003). ANChors away: an actin based mechanism of nuclear positioning. *J. Cell Sci.* **116**, 211-216.

Starr, D. A. and Fischer, J. A. (2005). KASH 'n Karry: the KASH domain family of cargo-specific cytoskeletal adaptor proteins. *BioEssays* **27**, 1136-1146.

Starr, D. A., Hermann, G. J., Malone, C. J., Fixsen, W., Priess, J. R., Horvitz, H. R. and Han, M. (2001). unc-83 encodes a novel component of the nuclear envelope and is essential for proper nuclear migration. *Development* **128**, 5039-5050.

Volk, T. (1992). A new member of the spectrin superfamily may participate in the formation of embryonic muscle attachments in Drosophila. *Development* **116**, 721-730.

Welte, M. A., Gross, S. P., Postner, M., Block, S. M. and Wieschaus, E. F. (1998). Developmental regulation of vesicle transport in Drosophila embryos: forces and kinetics. *Cell* **92**, 547-557.

Wilhelmsen, K., Litjens, S. H., Kuikman, I., Tshimbalanga, N., Janssen, H., van den Bout, I., Raymond, K. and Sonnenberg, A. (2005). Nesprin-3, a novel outer nuclear membrane protein, associates with the cytoskeletal linker protein plectin. *J. Cell Biol.* **171**, 799-810.

Yu, J., Starr, D. A., Wu, X., Parkhurst, S. M., Zhuang, Y., Xu, T., Xu, R. and Han, M. (2006). The KASH domain protein MSP-300 plays an essential role in nuclear anchoring during Drosophila oogenesis. *Dev. Biol.* **289**, 336-345.

Zhang, Q., Skepper, J. N., Yang, F., Davies, J. D., Hegyi, L., Roberts, R. G., Weissberg, P. L., Ellis, J. A. and Shanahan, C. M. (2001). Nesprins: a novel family of spectrin-repeat-containing proteins that localize to the nuclear membrane in multiple tissues. *J. Cell Sci.* **114**, 4485-4498.

Zhang, Q., Ragnauth, C., Greener, M. J., Shanahan, C. M. and Roberts, R. G. (2002). The nesprins are giant actin-binding proteins, orthologous to Drosophila melanogaster muscle protein MSP-300. *Genomics* **80**, 473-481.

Zhang, Q., Ragnauth, C. D., Skepper, J. N., Worth, N. F., Warren, D. T., Roberts, R. G., Weissberg, P. L., Ellis, J. A. and Shanahan, C. M. (2005). Nesprin-2 is a multi-isomeric protein that binds lamin and emerin at the nuclear envelope and forms a subcellular network in skeletal muscle. *J. Cell Sci.* **118**, 673-687.

Zhen, Y. Y., Libotte, T., Munck, M., Noegel, A. A. and Korenbaum, E. (2002). NUANCE, a giant protein connecting the nucleus and actin cytoskeleton. *J. Cell Sci.* **115**, 3207-3222.